Journal of Advances in Applied & Computational Mathematics, 2025, 29-30

Published by Avanti Publishers

Journal of Advances in Applied & Computational Mathematics

ISSN (online): 2409-5761

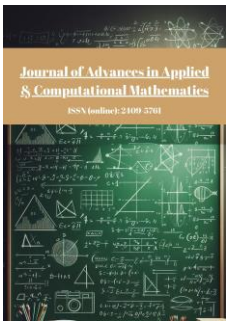

Mathematical Modelling of the Health Impact of Air Pollution from Figuil Cement and Marble Works on the Respiratory System of the Local Population

Kikmo Wilba Christophe* and Abanda Andre

National Higher Polytechnic School of Douala, University of Douala, Douala, Cameroon

ARTICLE INFO

Article Type: Research Article

Academic Editor: Faïçal Ndaïrou

Keywords:
Air pollution
Respiratory health
Industrial emissions
Mathematical modeling
Particulate matter ($PM_{2.5}$)

Timeline:
Received: May 06, 2025
Accepted: June 10, 2025
Published: June 25, 2025

Citation: Christophe KW, Andre A. Mathematical modelling of the health impact of air pollution from figuil cement and marble works on the respiratory system of the local population. J Adv Appl Computat Math. 2025; 12: 29-30.

DOI: https://doi.org/10.15377/2409-5761.2025.12.3

ABSTRACT

Air pollution notably stemming from cement and marble industries has been identified as a significant factor contributing to deteriorating respiratory health in regions of high industrial density. Figuil region in northern Cameroon suffers a disturbing health impact from industrial facilities emitting fine particulate matter and sulphur dioxide heavily. Quantitatively assessing effect of pollutants on health of local populations remains primary objective of this somewhat obscure study mercifully. A mathematical model derived from SEIR model incorporates atmospheric pollutant concentrations as environmental forcing variables rather effectively nowadays. Innovation here integrates environmental epidemiological and demographic data dynamically into a spatio-temporal modelling framework enabling fairly accurate estimation of various exposure risks. Numerical simulations revealed a statistically significant correlation between peaks in $PM_{2.5}/SO_2$ concentrations and increased cases of chronic bronchitis asthma and pneumonia during dry season. Regions near industrial sites show 2.8 times higher health risk compared with areas far away from such polluting facilities. Targeted public health interventions and industrial regulation are badly needed as underscored by these quite revealing data mercifully. Study proposes various mitigation measures including enhanced air quality monitoring around industrial sites and implementation of rather efficient filtration systems.

*Corresponding Author
Email: christopherkikmo@gmail.com
Tel: +(237) 673063916

1. Introduction

Cement production entails an arduous energy-intensive process resulting in copious emissions of pollutants during infrastructure construction nationwide every year. Rapid expansion besets cement industries in developing regions often fueling ecological degradation and public health issues amidst booming construction demands. Cement and marble works operates vigorously in FIGUIL situated roughly in northern Cameroon amidst prevalent industrial activity [1-3]. Climatic conditions and geography in the area greatly influence dispersion of pollutants particularly concentration of fine particles emitted by the plant into ambient air. Pollution may badly affect livelihoods of plant workers, farmers and local communities residing in this diverse region with varied population demographics. Cement production involves calcination and grinding of raw materials like limestone and clay resulting in generation of copious dust and noxious gas emissions [4-6]. Fossil fuels burning in cement kilns emits massive amounts of CO_2 into atmosphere thereby exacerbating climate change drastically. Populations near cement plants like the one operating in Figuil have been shown to suffer from alarmingly high levels of air pollution [7-9]. Elevated incidence of respiratory diseases and cardiovascular maladies occurs alongside heightened prevalence of cancer quite frequently nowadays [10-12]. Vegetation and waterways near a cement plant are subject to effects of particulate deposition quite frequently and rather drastically. Mathematical models assess impact of air pollution from cement and marble works in FIGUIL on respiratory health of nearby populations quite severely. Enforcement of rules intended to curb pollution from cement factories stays a hurdle especially in areas with scarce resources for oversight [2, 13-15]. Pollution from cement plant negatively impacts quality of life of local residents and swells health costs amidst economic growth in region. Pollution ravages local agriculture pretty badly leading to diminished crop yields and shaky food security nationwide over time somehow [7, 16-18]. Environmental epidemiological and demographic data will be amalgamated rather haphazardly in this somewhat eccentric study providing fairly accurate assessment of various health risks. Results of such studies will significantly inform development of public health policies aimed squarely at shielding vulnerable communities from egregious industrial pollution effects nationwide.

Figure 1: Illustrates the emissions of thick smoke and dust.

Fig. (**1**) starkly illustrates industrial activity's direct impact at Figuil cement plant with dense smoke and dust plume visibly emanating from production site. A thick column of atmospheric emissions signifies copious amounts of fine particulate matter like $PM_{2.5}$ and PM_{10} alongside polluting gases such as sulphur dioxide. Smoke's visual intensity serves as tangible proof of atmospheric overload with solid pollutants and gaseous emissions accumulating rapidly outdoors. Suspended particles from combustion of raw materials and clinker burning process disperse into local atmosphere affecting air quality breathed by local inhabitants heavily [12, 19, 20]. This illustration thus highlights not only perilous closeness between emission source and residential areas but also lack of effective filtration devices confirming public health concerns. Strong visual evidence justifying need for mathematical modelling surfaces pretty clearly anticipating dire long-term health consequences from pollution quite effectively.

Figuil town situated in northern Cameroon's Mayo-Louti department remains strategic owing largely to bordering Chad and Nigeria and boasting significant industrial activity. Tropical Sudano-Sahelian climate and seasonal water resources alongside savannah-type vegetation support economy based mainly on subsistence farming livestock and extractive industries [3, 21-23]. However, these industries are responsible for significant air pollution, characterised by the continuous emission of fine particles ($PM_{2.5}$, PM_{10}), sulphur dioxide (SO_2) and nitrogen oxides (NO_x), which seriously affect air quality, human health and the local environment. Developing an original mathematical model accurately assesses health impacts of air pollutants on populations living around Figuil cement plant and marble factory nearby [2, 24]. A modified SIR compartmental structure heavily influences proposed model formulation and it incorporates real environmental data quite effectively with epidemiological and demographic info. Traditional compartmental models often used for horizontally transmitted infectious diseases like influenza are unsuitable for simulating diseases caused by pollution [25, 26]. Existing atmospheric dispersion models are often coupled with statistical analyses but rarely with SIR-type human health dynamics models nowadays. Major innovation here manifests largely through development of some hybrid model accounting vertically for environmental transmission induced by industrial pollutant exposure [27, 28]. This model enables estimation of lung disease incidence and progression rates by merging pollutant concentration evolution with respiratory disease dynamics in a vulnerable populace. It signifies a rather substantial theoretical leap and operational improvement over extant methodologies providing some kinda decision-making gizmo for environmental stewardship in heavily industrialized locales.

2. The Transmission Pattern of Respiratory Diseases Around the Figuil Cement and Marble Works is Characterised by Vertical Transmission

Prevalence of respiratory diseases near Figuil cement and marble works can be attributed mostly to factors associated heavily with pollution from industrial activities. Cement and marble works activities generate fine particles and airborne pollutants that exacerbate respiratory health issues among surrounding populations quite significantly [29, 30]. A compartmental model for epidemiological modelling near Figuil cement and marble works requires categorizing population into discrete health states or exposure levels [31, 32]. Models frequently elucidate dynamics of infectious diseases but can be adapted cleverly for modeling impact of pollution rather haphazardly on human health. Model incorporates historical context of disease quite extensively in its formulation obviously referencing previous study number 10 [3, 33]. Age at initial infection impacts likelihood of chronic disease development later quite significantly in many cases apparently. Susceptible individuals must be divided into age classes thus necessitating such a categorization rather elaborately for various obvious reasons [34, 35]. A distributed system might emerge from envisaging a model that exists on a continuum rather sporadically with varying degrees of cohesion. Natural restriction to five age classes occurs given known data from a retrospective study around Figuil Cement and Marble Works in northern Cameroon. Compartments represent health states heavily influenced by exposure to various pollutants in an epidemiological context related to pollution [36, 37].

A model of respiratory disease transmission near Figuil cement and marble works is represented excluding vertical transmission mechanisms somehow graphically illustrated in Fig. (**2**). Ten distinct classes comprise it and five vulnerable compartments are presented therein somewhat awkwardly:

- The compartment designated as $\mathbf{S_1}$ encompasses the demographic cohort of infants and children aged 0 to 5 years. In this compartment, we have all the births of the total population, which is represented by the variable Λ.

A portion of these births, designated as pbC, will be directed to the chronic latent compartment. The infants who grow up with a $\mathbf{p_1}$ proportion will enter the $\mathbf{S_2}$ compartment. Additionally, the compartment includes infants who die with a proportion of $\mu\mathbf{S_1}$ and infants infected with a proportion $\boldsymbol{\beta_{1,i}}$ of vertical transmission (mother-to-child). These infants become latently infected $\mathbf{E_I}$ with probability $\boldsymbol{\alpha_1}$ and chronically latent $\mathbf{E_C}$ with probability $(1 - \boldsymbol{\alpha_1})$. Based on data from our retrospective study, we estimate that $(1 - \boldsymbol{\alpha_1}) = 70\%$.

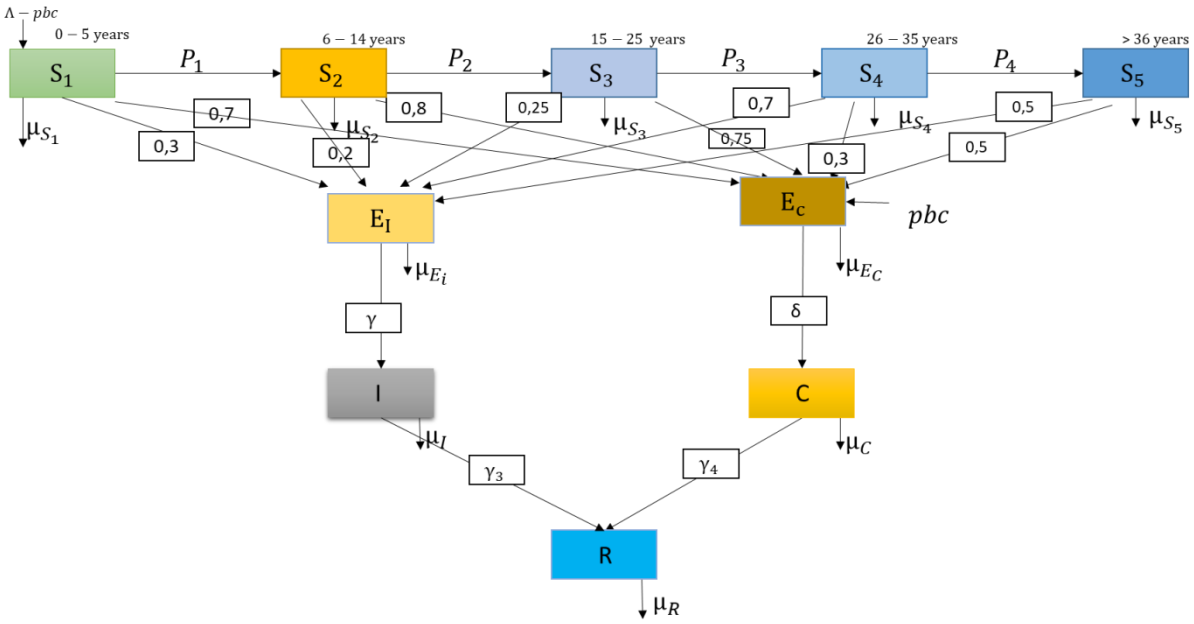

Figure 2: The respiratory disease transmission model in the vicinity of the Figuil cement and marble factory, with vertical transmission.

- The second compartment, $\mathbf{S_2}$, represents the demographic cohort of children aged 6 to 14. In this compartment, children from compartment $\mathbf{S_1}$ with a proportion $\mathbf{p_1}$ enter, and children who grow up with a proportion $\mathbf{p_2}$ enter compartment $\mathbf{S_3}$. Additionally, those who have become infected with a coefficient $\boldsymbol{\beta_{2,i}}$ dependent on the infectant are included in this compartment. The mortality rate in this compartment is $\mu\mathbf{S_2}$; it is also worth noting that in the outflow, there are susceptible individuals from compartment S_2 who have been in contact with the disease and have become latent infected $\mathbf{E_I}$ (i.e., who will evolve towards an infected state) with probability $\boldsymbol{\alpha_2}$ and chronic latent $\mathbf{E_C}$ with probability $(1 - \boldsymbol{\alpha_2})$.
- The compartment $\mathbf{S_3}$ represents the population of adults aged 15 to 25. The input to this compartment consists of children who have been raised in compartment $\mathbf{S_2}$ with a proportion $\mathbf{p_2}$. The output is composed of $\mu\mathbf{S_3}$ mortality; children who have been raised with a proportion $\mathbf{p_3}$ and individuals who have not been infected but are susceptible to infection with a proportion $\boldsymbol{\beta_{3,i}}$, which depends on the infectant.
- The demographic cohort represented by Compartment $\mathbf{S_4}$ is adults aged between 26 and 35 years. The inflow to this compartment is comprised of adults who have been raised in compartment $\mathbf{S_4}$, with a proportion $\mathbf{p_3}$. The outflow from this compartment consists of adults who mature and transition to compartment $\mathbf{S_5}$, with a proportion of $\mathbf{p_4}$ representing the $\mu\mathbf{S_4}$ mortality of the susceptible. It is also noteworthy that the susceptible individuals who are infected exhibit a proportion $\boldsymbol{\beta_{4,i}}$ that is dependent on the infectant. These individuals transition into the compartment of infected latents $\mathbf{E_I}$ with a probability of $\boldsymbol{\alpha_4}$ and the chronic latent $\mathbf{E_C}$ compartment with a probability of $(1 - \boldsymbol{\alpha_4})$.
- The population of compartment $\mathbf{S_5}$ is comprised of individuals over the age of 36, adolescents, and those deemed susceptible. The inflow to this compartment is represented by $\mathbf{p_4S_4}$, which denotes the proportion of adults who have grown up in compartment $\mathbf{S_4}$. The outflow is the $\mu\mathbf{S_5}$ mortality of susceptible and infected individuals who become infected with the proportion $\boldsymbol{\beta_{4,i}}$, which depends on the infectant. This flow enters compartment $\mathbf{E_I}$ with a probability of $\boldsymbol{\alpha_5}$ and compartment $\mathbf{E_C}$ with the complementary probability of $(1 - \boldsymbol{\alpha_5})$. The division of the susceptible population into five compartments provides a reasonable approximation to the reality of pollution-

related epidemiology, given that the prognosis for disease progression depends on the age at which the disease is contracted.

Two distinct compartments of latent have been identified.

- The fifth compartment, designated $\mathbf{E_I}$, represents infectious latents, that is, those that will evolve towards an infectious state. The input to this compartment is characterized by susceptible individuals who have been infected in proportions $\boldsymbol{\alpha_i\beta_{i,j}}$. The output is constituted by two elements: firstly, the mortality $\mu\mathbf{E_I}$, and secondly, the evolution towards an infectious state with a proportion $\boldsymbol{\gamma}$.
- The second compartment, $\mathbf{E_C}$, represents chronic latents $\mathbf{E_C}$, i.e. latents that will evolve towards a chronic state. The output flow is constituted by the mortality $\mu\mathbf{E_C}$ and the evolution towards the chronic state with the proportion $\boldsymbol{\gamma}$. The infected compartment I is characterized by an input $\boldsymbol{\gamma}\mathbf{E_I}$ and an output comprising mortality (a natural mortality and a mortality due to the disease). The input to this compartment is represented by μI and recovery $\boldsymbol{\gamma_3}\mathbf{I}$.

The output of Compartment C is composed of mortality (natural mortality and mortality due to disease) μ_C and cure $\boldsymbol{\gamma_4}\mathbf{I}$. The input to this compartment is represented by $\boldsymbol{\delta}\mathbf{E_C}$.

The compartment designated as "R" represents those who have recovered from health problems.

It is assumed that the rate of general recruitment remains constant. It is assumed that chronicles participate with quantity (1 - p)bC to their number (or density) at births, with a proportion pbC going to chronicles. The introduction of vertical transmission reduces the number of births by a quantity pbC, which no longer becomes susceptible because the babies born from these births become chronic with the vertical transmission. This quantity pbC appears at the level of $\mathbf{E_C}$, leading to the following differential system:

$$
\begin{cases}
\dot{S}_1 = \Lambda - \mu_1 S_1 - \beta_{1,1} E_I S_1 - \beta_{1,2} E_C S_1 - \beta_{1,3} I_3 S_1 - \beta_{1,4} I_4 S_1 - p_1 S_1 - pbI_4 \\
\dot{S}_2 = p_1 S_1 - \mu_2 S_2 - \beta_{2,1} E_I S_2 - \beta_{2,2} E_C S_2 - \beta_{2,3} I_3 S_2 - \beta_{2,4} I_4 S_2 - p_2 S_2 \\
\dot{S}_3 = p_2 S_2 - \mu_3 S_3 - \beta_{3,1} E_I S_3 - \beta_{3,2} E_C S_3 - \beta_{3,3} I_3 S_3 - \beta_{3,4} I_4 S_3 - p_3 S_3 \\
\dot{S}_4 = p_3 S_3 - \mu_4 S_4 - \beta_{4,1} E_I S_4 - \beta_{4,2} E_C S_4 - \beta_{4,3} I_3 S_4 - \beta_{4,4} I_4 S_4 - p_4 S_4 \\
\dot{S}_5 = p_4 S_4 - \mu_5 S_5 - \beta_{5,1} E_I S_5 - \beta_{5,2} E_C S_5 - \beta_{5,3} I_3 S_5 - \beta_{5,4} I_4 S_4 \\
\dot{E}_I = \alpha_1 (\beta_{1,1} E_I S_1 + \beta_{1,2} E_C S_1 + \beta_{1,3} I_3 S_1 + \beta_{1,4} I_4 S_1) + \cdots \\
\quad + \alpha_2 (\beta_{2,1} E_I S_2 + \beta_{2,2} E_C S_2 + \beta_{2,3} I_3 S_2 + \beta_{2,4} I_4 S_2) + \cdots \\
\quad + \alpha_3 (\beta_{3,1} E_I S_3 + \beta_{3,2} E_C S_3 + \beta_{3,3} I_3 S_3 + \beta_{3,4} I_4 S_3) + \cdots \\
\quad + \alpha_4 (\beta_{4,1} E_I S_4 + \beta_{4,2} E_C S_4 + \beta_{4,3} I_3 S_4 + \beta_{4,4} I_4 S_4) + \cdots \\
\quad + \alpha_4 (\beta_{5,1} E_I S_5 + \beta_{5,2} E_C S_5 + \beta_{5,3} I_3 S_5 + \beta_{5,4} I_4 S_4) - \mu_E E_I - \gamma_i E_I \\
\dot{E_C} = (1-\alpha_1)(\beta_{1,1} E_I S_1 + \beta_{1,2} E_C S_1 + \beta_{1,3} I_3 S_1 + \beta_{1,4} I_4 S_1) + \cdots \\
\quad + (1-\alpha_2)(\beta_{2,1} E_I S_2 + \beta_{2,2} E_C S_2 + \beta_{2,3} I_3 S_2 + \beta_{2,4} I_4 S_2) + \cdots \\
\quad + (1-\alpha_3)(\beta_{3,1} E_I S_3 + \beta_{3,2} E_C S_3 + \beta_{3,3} I_3 S_3 + \beta_{3,4} I_4 S_3) + \cdots \\
\quad + (1-\alpha_4)(\beta_{4,1} E_I S_4 + \beta_{4,2} E_C S_4 + \beta_{4,3} I_3 S_4 + \beta_{4,4} I_4 S_4) + \cdots \\
+ (1-\alpha_5)(\beta_{5,1} E_I S_5 + \beta_{5,2} E_C S_5 + \beta_{5,3} I_3 S_5 + \beta_{5,4} I_4 S_4) - \mu_I E_I - \gamma_C E_C + pbI_4 \\
\dot{I}_3 = \gamma_i E_I - (\mu_I + \gamma_3) I_3 \\
\dot{I}_4 = \gamma_C E_C - (\mu_C + \gamma_4) I_4 \\
\dot{R} = \gamma_3 I_3 - \gamma_4 I_4 - \mu R
\end{cases}
\tag{1}
$$

Analyzing respiratory disease transmission model around Figuil cement and marble works involves calculating disease-free equilibrium point and basic reproduction number R_0 first necessarily. Stability of this equilibrium point will be studied subsequently with utmost care and rigor in forthcoming discussions. Given differential system's intricacy notwithstanding it can be encapsulated quite succinctly as follows:

$$\begin{cases} \dot{S}_1 = \Lambda - \mu_1 S_1 - \sum_{j=1}^{4} \beta_{1,j} I_j S_1 - p_1 S_1 - pbI_4 \\ \dot{S}_2 = p_1 S_1 - \mu_2 S_2 - \sum_{j=1}^{4} \beta_{2,j} I_j S_2 - p_2 S_2 \\ \dot{S}_3 = p_2 S_2 - \mu_3 S_3 - \sum_{j=1}^{4} \beta_{3,j} I_j S_3 - p_3 S_3 \\ \dot{S}_4 = p_3 S_3 - \mu_4 S_4 - \sum_{j=1}^{4} \beta_{4,j} I_j S_4 - p_4 S_4 \\ \dot{S}_5 = p_4 S_4 - \mu_5 S_5 - \sum_{j=1}^{4} \beta_{5,j} I_j S_5 \\ \dot{E_I} = \sum_{i=1}^{5} \alpha_i \sum_{j=1}^{4} \beta_{i,j} I_j S_i - \mu_E E_I - \gamma_i E_I \\ \dot{E_C} = \sum_{i=1}^{5} (1-\alpha_i) \sum_{j=1}^{4} \beta_{i,j} I_j S_i - \mu_I E_I - \gamma_C E_C + pbI_4 \\ \dot{I}_3 = \gamma_i E_I - (\mu_I + \gamma_3) I_3 \\ \dot{I}_4 = \gamma_C E_C - (\mu_C + \gamma_4) I_4 \\ \dot{R} = \gamma_3 I_3 - \gamma_4 I_4 - \mu R \end{cases} \quad (2)$$

Table 1: Description of model parameters.

Setting	Description	Value (Example or Estimated)	Dimension / Unit
Λ	Recruitment rate (births)	1000 individuals/year	individuals/year
pbC	Proportion of births affected by chronic vertical transmission	0.3	-
p_1	Proportion of children moving from S_1 to S_2	0.85	-
p_2	Proportion of young people moving from S_2 to S_3	0.9	-
p_3	Proportion of young adults moving from S_3 to S_4	0.95	-
p_4	Proportion of mature adults transitioning from S_4 to S_5	0.98	-
μ	Natural mortality rate	0.01	1/year
$\boldsymbol{\beta_{ij}}$	Transmission rate between susceptible classes S_i and infectious j	0.0005 à 0.01	1/(individual·year)
$\boldsymbol{\alpha_i}$	Proportion of newly infected becoming latently infectious (E_I)	0.3 à 0.5	-
$\boldsymbol{\gamma}$	Rate of progression of latent infections (E_I) to I_3	0.2	1/year
$\boldsymbol{\gamma_C}$	Rate of progression of chronic latents (E_C) towards I_4	0.1	1/year
$\boldsymbol{\gamma_3}$	Recovery rate of infected I_3	0.15	1/year
$\boldsymbol{\gamma_4}$	Cure rate of chronic I_4	0.05	1/year
μ_E	Mortality rate of latent infections	0.01	1/year
μ_C	Chronic mortality rate	0.02	1/year
μ_R	Mortality rate of those cured	0.005	1/year

2.1. Calculation of the Infection-Free Equilibrium Point (DFE)

The DFE is reached when $\boldsymbol{E_I = E_C = I_3 = I_4 = 0}$. Under the assumption that the populations of susceptible $\boldsymbol{S_i}$ are in their equilibrium state, we can express the following:

$$\Lambda - \mu_i S_i - p_i S_i = 0 \ \forall i = 1, \ldots, 5 \text{ thus } S_i^* = \frac{\Lambda}{\mu_i + p_i}$$

2.2. Investigation Into the Stability of the Infection-Free Equilibrium Point (DFE)

The number of basic reproductions, $\boldsymbol{R_0}$, is determined by the spectrum of the Jacobian matrix evaluated at the DFE. This matrix is formed by linearizing the system around the DFE.

Let F be the new infection rate matrix, given by:

$$F = \begin{pmatrix} \sum_{i=1}^{5} \alpha_i \beta_{i,1} S_i^* & \sum_{i=1}^{5} \alpha_i \beta_{i,2} S_i^* & \sum_{i=1}^{5} \alpha_i \beta_{i,3} S_i^* & \sum_{i=1}^{5} \alpha_i \beta_{i,4} S_i^* \\ \sum_{i=1}^{5} (1-\alpha_i) \beta_{i,1} S_i^* & \sum_{i=1}^{5} (1-\alpha_i) \beta_{i,2} S_i^* & \sum_{i=1}^{5} (1-\alpha_i) \beta_{i,3} S_i^* & \sum_{i=1}^{5} (1-\alpha_i) \beta_{i,4} S_i^* \\ 0 & 0 & 0 & 0 \\ 0 & 0 & 0 & 0 \end{pmatrix}$$

Additionally, the transition rate matrix between infected compartments is represented by :

$$V = \begin{pmatrix} \mu_E + \gamma_I & 0 & 0 & 0 \\ 0 & \mu_C + \gamma_C & -pb & 0 \\ -\gamma_I & 0 & \mu_I + \gamma_3 & 0 \\ 0 & -\gamma_C & 0 & \mu_C + \gamma_4 \end{pmatrix}$$

Accordingly, the number of basic reproductions is given by $\boldsymbol{R_0 = \rho(-FV^{-1})}$ or $\boldsymbol{\rho(A)}$, the spectral radius of the matrix A, that is, the dominant eigenvalue defined if $\boldsymbol{S_P}$(A) represents the spectrum of A. The eigenvalues of $\boldsymbol{-FV^{-1}}$ are the solutions of the characteristic equation: $\det(\boldsymbol{-FV^{-1} - \lambda I}) = \boldsymbol{0}$, thus the expression of $\boldsymbol{R_0}$ can be approximated by:

$$R_0 \approx max \left\{ \frac{\sum_{i=1}^{5} \alpha_i \beta_{i,1} S_i^*}{\mu_E + \gamma_I}, \ \frac{\sum_{i=1}^{5} \alpha_i \beta_{i,2} S_i^*}{\mu_C + \gamma_C}, \ \frac{\sum_{i=1}^{5} \alpha_i \beta_{i,3} S_i^*}{\mu_I + \gamma_3}, \ \frac{\sum_{i=1}^{5} \alpha_i \beta_{i,4} S_i^*}{\mu_C + \gamma_4} \right\}$$

2.3. Investigation Into the Stability of the Infection-free Equilibrium Point (DFE)

In order to study the stability of the DFE, it is necessary to analyze the eigenvalues of the Jacobian matrix of the system evaluated at the DFE [38, 39, 40]. If all the eigenvalues have negative real parts, the DFE is locally asymptotically stable [9]. This will be demonstrated to be the case when $\boldsymbol{R_0 \leq 1}$.

The Jacobian of system (1) evaluated at the disease-free equilibrium is given by $\boldsymbol{J(0) = F + V}$. Since F is non-negative and V is a stable Metzler matrix, F + V represents a regular decomposition of J(0). Therefore, in accordance with [5, 41, 42], we may conclude that $\boldsymbol{\rho(-FV^{-1})}$ is equivalent to It can be shown that α(F + V) < 0, where α(M) represents the stability modulus of the matrix M, defined as the largest real part of the elements of its spectrum. Consequently, the disease-free equilibrium is locally asymptotically stable. This, in turn, implies, in accordance with Hirsch's theorem, that the disease-free equilibrium (in this case, the origin) is globally asymptotically stable if $\boldsymbol{R_0 = \rho(-FV^{-1}) < 1}$.

2.4. Parameter Identification

Our survey recorded live births of women and some associated characteristics such as sex age and survival status alongside age at death. Prevalence among people living near Figuil cement and marble factory is estimated by some public health professionals to be roughly eighteen percent. Program managers estimate eighty-five percent of population faces risk of contamination heavily nowadays across various regions. Crude birth rate in vicinity of cement and marble works is estimated at 51 per thousand inhabitants roughly. Mortality rate stands at roughly 11 per thousand inhabitants overall. 52 out of every 1000 individuals residing near cement plant died sometime

between 2012 and 2018 apparently in that vicinity 35 per thousand youngsters under 5 years old are included in this figure and 26 per thousand kids between 6 and 14 are too. Mortality rate stood at 63 per thousand among adults aged 25 and above largely. Mortality risk between birth and age five was roughly estimated at 121 per 1000 live births equating to over one in ten kids dying young [1, 43, 44]. Mortality indicators presented here derive from birth history data retrospectively collected with considerable rigor and sometimes questionable accuracy. Health professionals evaluated likelihood of progression quite accurately based on age at infection occurrence pretty effectively. Aforementioned assessment manifests graphically below showing decline in estimated probability of transitioning into chronicity with increasing age quite markedly (Fig. **3** and **4**, Table **2**).

Table 2: The data set comprises infant mortality rates for the period 2012-2018 [1].

Age Groups	Mortality Rate Per 1000 in the Same Age Groups	Source
Under 5 years old	12	[2]
6 to 14 years old	26	[2]
15 to 25 years old	34	[2]
Over 25 years old	63	[2]

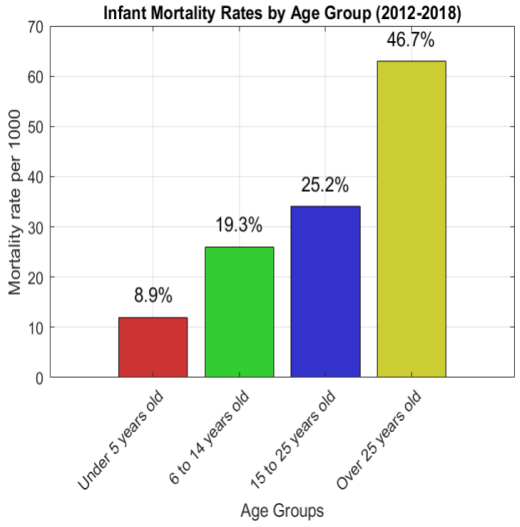

Figure 3: The risk of progression to chronic carriage is contingent upon the age of infection.

Figure 4: Death rates by age groups (2012-2018).

Data indicate probability of transitioning into chronic respiratory infection being fivefold higher in kids under five than those over 25 years old. We assembled parameters from historical data to develop a quirky model of respiratory infection transmission pretty effectively it seems [1, 45]. Parameters are presented subsequently in Table **3**.

Table 3: Description of model parameters with estimated values and dimensions.

Parameter	Description	Estimated Value	Dimension (Unit)
ρ	Relative infection strength of chronic infections compared to acute	0.16	Dimensionless
γ_1	Transition (pass-through) rate from latent to infectious state	6	per year (year^{-1})
γ_3	Healing rate of acute infectious individuals	4.8	per year (year^{-1})
γ_4	Chronic infection rate (from chronic latents to chronic cases)	0.023	per year (year^{-1})
β_1	Strength of infection for children aged 0 to 5	0.159	per year (year^{-1})
β_2	Strength of infection for children aged 6 to 14	0.144	per year (year^{-1})
β_3	Strength of infection for individuals aged 15 to 25	0.116	per year (year^{-1})
β_4	Strength of infection for individuals over age 25	0.030	per year (year^{-1})

Table 4: Population density.

District	Population Estimates	Density (hab/km²)	Factory *Proximity* (km)
Figuil Centre	8,000	1,200	1.0
Peripheral area	5,000	600	3.5
Rural areas	3,500	250	5.5

Table 5: Annual average pollutant concentrations.

Pollutant	Mean Concentration	Unit	WHO *Limit*
PM2.5	25	µg/m³	15
SO_2	8	µg/m³	20
NOx	15	µg/m³	40

Table 6: Local estimates of the prevalence of respiratory diseases.

Age Range	Prevalence (%) of Respiratory Diseases
Children < 5 years	7.0
Adults 18-60.	4.5
seniors	10.0

Table 7: Epidemiological model parameters.

Parameter	Symbol	Value	Unit	Rationale / Source
Transfer rate	β	0.0018	—	Calibrated from local studies
Incubation time	$1/\sigma$	4	days	Epidemiological literature from the region
Infectious time	$1/\gamma$	10	days	Regional clinical data
Total population	N	16,500	residents	Sum of neighbourhoods and census.

Table 8: Epidemiological and environmental parameters used for modelling in Figuil.

Item	Value/Source
Population totale (N)	16 500
Density/Factory distance.	1200 hab/km² at 1 km (Figuil centre)
PM2.5 annual mean	25 µg/m³ (above WHO norm: 15 µg/m³)
acute infection cure rate	γ = 4.8 years⁻¹
chronic infection rate	γc = 0.023 years⁻¹
Transfer rate	β = 0.0018 (locally adjusted)
Infection rate by age group	[0.159, 0.144, 0.116, 0.030]

A thorough review of the literature highlights a consistent trend: the force of infection decreases progressively with age across most epidemiological studies. Specifically, the infection force is estimated at 0.159 among children under 5 years old, then declines to 0.144 for those aged 5 to 14, and continues to diminish in older groups. These values align with recent data and publications focusing on respiratory diseases, from which the estimates presented in the following table are derived. The distribution of carriage and epidemiological burden of respiratory infections has been assessed heterogeneously across age brackets in several comprehensive studies [3, 46, 47]. This stratified approach is justified within the framework of our model, which investigates the transmission dynamics of respiratory illnesses and the associated health impacts of air pollution near the Figuil cement and marble industries. Furthermore, the model accounts for possible age-specific susceptibility and vertical transmission mechanisms, reinforcing the relevance of this segmented estimation.

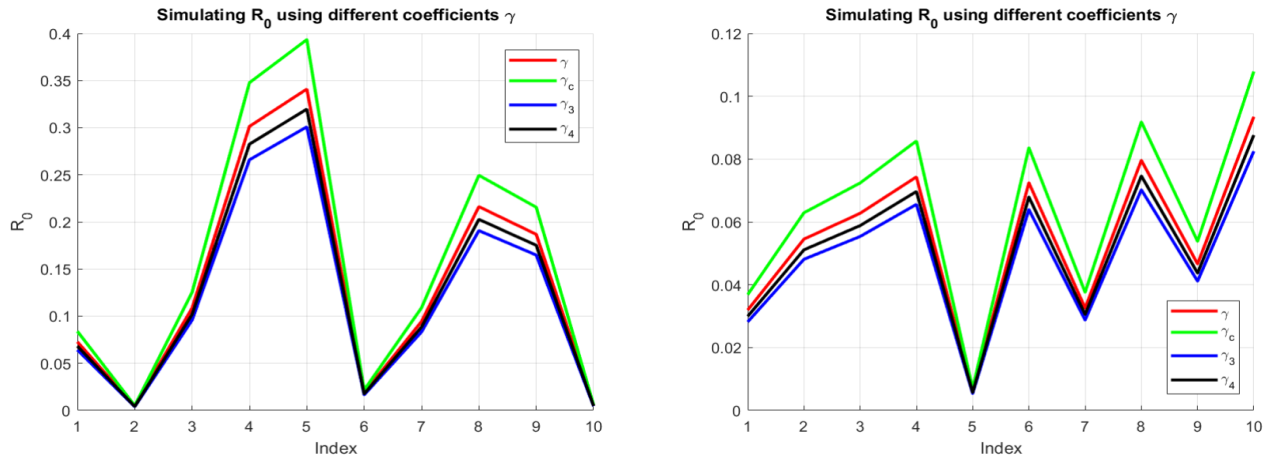

Figure 5: Impact of parameters on the dynamics of the system: variation of R0 with γ, γ_c, γ_3, and γ_4.

In Fig. (**5**). the R_0 curve demonstrates the impact of the parameters γ, γ_c, γ_3, and γ_4 on the system's dynamic behaviour. As these parameters increase, the denominator (µ+γ, µ+ γ_c, . . .) becomes larger, which results in a reduction of R_0. This demonstrates that the system exhibits greater resilience or reduced susceptibility to external influences. Conversely, a decline in these parameters leads to an increase in R_0, indicating that interactions of the form $a_i \beta_i S_i$ exert a more pronounced influence on the system. The curves illustrate that R_0 is higher in instances of low attenuation (as observed in the case of γ) and lower in scenarios of high attenuation (such as γ_4).

3. Pollution Model Linked to Respiratory Disease Transmission Near FIGUIL Cement and Marble Works

Epidemiological transmission dynamics are integrated into pollution model framework at local level coupling with respiratory disease transmission quite intricately [48-50]. Additional variables and parameters adapted

specifically for factoring in air pollution's impact on respiratory disease transmission progression are employed alongside previously defined ones. Additional variables and parameters crucial for model formulation are introduced subsequently in next section with requisite details thoroughly.

- P(t) : Concentration of fine particles (PM2.5, PM10) at time t.
- $\mathbf{SO_2}$(t): The concentration of sulfur dioxide (SO_2) at a specific point in time (t).
- $\mathbf{NO_x}$(t): The concentration of nitrogen oxide ($\mathbf{NO_x}$) at a specific point in time (t).
- E(t) : The degree of population exposure to pollutants at a specific point in time (t).
- S(t) : The number of individuals presenting with respiratory illnesses at a specific point in time (t).
- V(t): The number of cases in which vertical transmission of pollution impacts has occurred in newborns at a specified point in time (t) is indicated.
- $\boldsymbol{\alpha, \beta, \gamma}$: The parameters represent the conversion rates from pollutant concentrations to exposure levels.
- $\boldsymbol{\delta, \epsilon, \zeta}$: The parameters represent the incidence rates of respiratory diseases and cases of vertical transmission.

Pollutant concentrations are modeled in accordance with industrial emissions and atmospheric dispersion processes.

$$\begin{cases} \dfrac{dP(t)}{dt} = f_P(t) - k_P P(t) \\ \dfrac{dSO_2(t)}{dt} = f_{SO_2(t)}(t) - k_{SO_2} SO_2(t) \\ \dfrac{dNO_x(t)}{dt} = f_{NO_x(t)}(t) - k_{NO_x} NO_x(t) \end{cases} \tag{3}$$

The emission rates of the pollutants, $\mathbf{f_P}$(t), $\mathbf{f_{SO_2(t)}}$(t), and $\mathbf{f_{NO_x(t)}}$(t) are functions of time, as are the dispersion and natural degradation coefficients of the pollutants, $\mathbf{k_P}$, $\mathbf{k_{SO_2}}$, and $\mathbf{k_{NO_x}}$.

3.1. A critical Examination of the Model, with Particular Attention to Its Stability

The equations for each pollutant are of the form $\frac{\mathbf{dC(t)}}{\mathbf{dt}} = \mathbf{f_C(t)} - \mathbf{k_C C(t)}$, where C(t) represents the pollutant concentration, $\mathbf{f_C(t)}$ is the emission rate, and $\mathbf{k_C}$ is the dispersion and degradation coefficient. These equations are non-homogeneous first-order linear differential equations, for which the general solution can be found using either analytical or numerical methods. The general solution of the equation $\frac{\mathbf{dC(t)}}{\mathbf{dt}} = \mathbf{f_C(t)} - \mathbf{k_C C(t)}$ is found using the integrating factor $\boldsymbol{\mu(t) = e^{\int k_C dt} = e^{k_C t}}$.

We have: $e^{k_C t}\left(\frac{dC(t)}{dt} + k_C C(t)\right) = e^{k_C t} f_C(t)$

$\Leftrightarrow \frac{d}{dt}\left(e^{k_C t} C(t)\right) = e^{k_C t} f_C(t)$

$\Leftrightarrow e^{k_C t} C(t) = \int e^{k_C t}\, f_C(t)dt + C_0$ where C_0 is the integration constant.

$\Leftrightarrow C(t) = e^{-k_C t}\left(\int e^{k_C t}\, f_C(t)dt + C_0\right)$

Plant production stays fairly steady overall but fluctuates somewhat erratically due largely to demand shifts and periodic equipment overhauls. Linear models are apt in such scenarios with formulation $\mathbf{f_C(t) = a + bt}$ being decently representative. Usefulness of model lies in assumption that pollutant emissions rise gradually over time owing to equipment degradation and dwindle somewhat due to emission-reducing interventions. Interval [0 T] spans time period over which integral gets calculated slowly. $\mathbf{C(t) = e^{k_C(T-t)}\left(\frac{a+b(Tk_C-1)}{{k_C}^2}\right) + e^{-k_C t}\left(\frac{b}{{k_C}^2} - \frac{a}{k_C} + C_0\right)}$.

3.1.1. Interpretation

- In the event that the emission terms are constant ($\mathbf{f_C(t) = f_0}$), the equilibrium value of C(t) will approach $\mathbf{C_\infty = \frac{f_0}{k_C}}$ over time.

- The dispersion and degradation coefficients ($\mathbf{k_C}$) indicate the rate of dispersion and degradation, respectively. A higher $\mathbf{k_C}$ signifies a more rapid reduction in the concentration of C(t). The objective is to examine the behavior of small perturbations around $\mathbf{C}_\infty$. To this end, we assume a small perturbation ϵ(t) such that C(t) can be expressed as $\mathbf{C(t)} = \mathbf{C}_\infty + \boldsymbol{\epsilon}(\mathbf{t})$. we have:

$$\frac{d}{dt}(C_\infty + \epsilon(t)) = f_0 - k_C(C_\infty + \epsilon(t))$$

$$\Leftrightarrow \frac{d\epsilon(t)}{dt} = f_0 - k_C\left(\frac{f_0}{k_C} + \epsilon(t)\right)$$

$$\Leftrightarrow \frac{d\epsilon(t)}{dt} = -k_C\epsilon(t).$$

The general solution to this first-order linear differential equation is given by $\boldsymbol{\epsilon}(\mathbf{t}) = \boldsymbol{\epsilon_0}\, \mathbf{e}^{-\mathbf{k_C t}}$, where $\boldsymbol{\epsilon_0}$ represents the initial disturbance.

3.1.2. Stability Analysis

In the event that $\mathbf{k_C}$ is positive, the disturbance ϵ(t) declines exponentially in accordance with the passage of time. This indicates that the $\mathbf{C}_\infty = \frac{\mathbf{f_0}}{\mathbf{k_C}}$ equilibrium is globally stable, as any initial disturbance attenuates over time.

In the context of pollutant dispersion and degradation, the scenario in which $\mathbf{k_C}$ is negative is not physically realistic. This is because $\mathbf{k_C}$ represents natural dispersion and degradation, which are always positive.

The model demonstrates overall stability for each pollutant, provided that the dispersion and degradation coefficients ($\mathbf{k_C}$, $\mathbf{k_{SO_2}}$, $\mathbf{k_{NO_x}}$) are positive. In practice, this implies that pollutant concentrations will tend towards stable long-term values, determined by emission rates and dispersion/degradation coefficients. This stability ensures that concentrations do not diverge indefinitely, thereby facilitating effective management and prediction of pollution levels.

The level of exposure of the population to pollutants is dependent upon the concentration of said pollutants

$$E(t) = \alpha P(t) + \beta\, SO_2(t) + \gamma\, NO_x(t)E(t).$$

The potential impact of respiratory diseases and vertical transmission on human health is modelled by:

$$\begin{cases} \dfrac{dS(t)}{dt} = \delta E(t) - \mu S(t) \\ \dfrac{dV(t)}{dt} = \epsilon E(t) - \nu V(t) \end{cases} \tag{4}$$

In this model, μ and ν represent the recovery or mortality rates for respiratory disease and vertical transmission cases, respectively. The initial conditions are assumed to be given by $\mathbf{S(0)} = \mathbf{S_0}$ and $\mathbf{V(0)} = \mathbf{V_0}$, where $\mathbf{S_0}$ and $\mathbf{V_0}$ are the initial populations at t=0. The E(t) functions are assumed to be known or estimated from environmental data (e.g., pollutant concentration in air).

3.2. Results Numerical Simulation

Numerical simulations conducted here facilitate spatial and temporal modelling of atmospheric pollutant dispersion particularly fine particles PM10 and sulphur dioxide emitted by industrial facilities in Figuil. Fig. (**6**) presents a high-resolution map of PM10 concentrations around those sites revealing significant spatial heterogeneity correlated with local configuration and prevailing winds from various emission sources nearby. Fig. (**7**) illustrates temporal evolution of various pollutant concentrations and potential health impacts under daily variability in emissions and meteorological conditions. Results enable assessment of high exposure areas and varied effects on population health depending on exposure nature and varying intensity quite differently. This provides essential basis for environmental risk analysis and informs policy-making greatly under varying conditions normally.

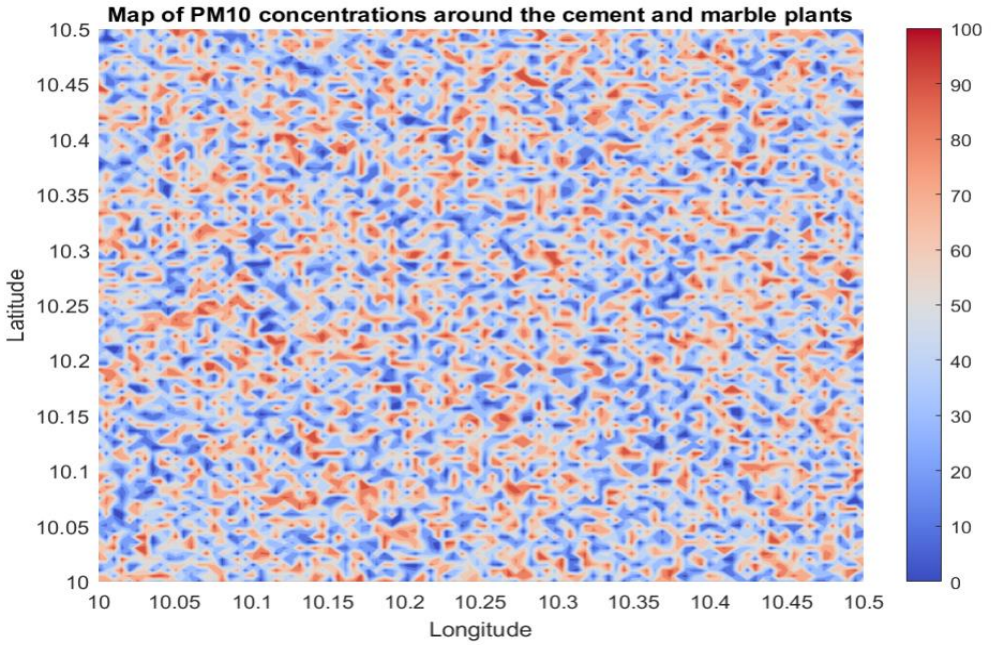

Figure 6: A map of the concentration of PM10 particles in the vicinity of the FIGUIL Cement and Marble Works is provided herewith.

Fig. (**6**) depicts PM10 fine particle concentration spatially around cement and marble factories in Figuil area pretty clearly somehow. Air pollution levels exhibit a sporadic distribution fluctuating wildly from sparse concentrations in blue zones to dense red hotspots exceeding 90 µg/m³ locally. Significant health risks plague local populations due largely in part to concentrations that greatly surpass WHO daily standards of 50 µg/m³ for respiratory and cardiovascular diseases. Observed distribution can be partly explained by local topography and meteorological conditions like dominant winds and atmospheric stability alongside industrial emissions from multiple sources. Map relies heavily on spatial snapshot lacking temporal context thereby severely limiting inferences regarding chronic exposure quite substantially over time. Absence of longitudinal data namely data tracking progression of phenomenon over time poses significant challenge in rigorously evaluating long-term implications of pollution on public health. Potential health outcomes gathered from hospital records in low-resource settings may be plagued by underreporting bias or grossly inaccurate diagnoses sometimes. An integrated epidemiological approach based on cohort studies or longitudinal follow-ups would be more suitable here for establishing robust causal links between exposure to PM10 and observed pathologies. Integrating mapping with georeferenced sensors and scientifically validated models like AERMOD enhances prediction of actual human exposure quite remarkably. Fig. (**6**) serves as vital environmental diagnostic tool but further methodological and epidemiological development must occur effectively guiding risk reduction policies in Figuil industrial areas.

Fig. (**7**) comprises two graphs highlighting a dynamic and somewhat fraught relationship between air pollution from industrial sources and resultant public health issues. First graph tracks air pollutant concentration changes remarkably over time and second illustrates health effects observed in population very gradually. Air quality degradation correlates temporally with a sharp increase in respiratory diseases underscoring a crucial role for vigilant environmental monitoring in preventing disease. Top graph illustrates temporal evolution of concentration of several air pollutants including fine particles PM2.5 and PM10 sulphur dioxide SO_2 and nitrogen oxides NO_x. Dominant pollutant probably PM2.5 exhibits erratic fluctuations with pronounced spikes suggesting sporadic industrial pollution heavily influenced by factory activity fluctuations or weird weather conditions like thermal inversion and gusty winds. Ultrafine particles pose significant danger by deeply penetrating respiratory tracts and sparking inflammation of lung tissue and exacerbating cardiovascular disease severely. SO_2 and NO_x emissions contribute significantly to acid rain formation and tropospheric ozone buildup aggravating chronic respiratory issues like asthma and COPD pretty badly. Pollution's impact on human health is starkly reflected below through clinical data gathered quietly in local facilities. Respiratory disease consultations and hospitalisations surge in

tandem with pollutant concentration peaks albeit with a brief delayed reaction. Latency duration manifests as incubation period or pathological effects become apparent after exposure. These health data should be interpreted cautiously as they often emanate from low-resource settings with surveillance systems plagued by underreporting and inexact diagnoses. Data presented here likely stem from a cross-sectional study thereby severely limiting possibilities for causal inference in hindsight obviously. Robust confirmation of chronic effects from exposure stems largely from meticulously structured lengthy studies or cohort analyses undertaken painstakingly over time. Juxtaposition of two graphs starkly highlights a direct relationship between pollutant emissions and rather severe health consequences nationwide. Industrial pollution poses quite a grave public health emergency rather than just being an environmental issue obviously nowadays. Proactive air quality management averts further decrepitude of health in exposed populations quite rigorously and very effectively every year. Stricter regulation of industrial emissions is implied alongside implementation of real-time sensor systems and predictive models based on artificial intelligence. Targeted screening campaigns for vulnerable groups like children and elderly patients with comorbidities are also necessitated pretty urgently. Fig. (**7**) offers a stark visual distillation of links between environmental dynamics and harsh clinical reality quite effectively overall. Scientists and industry need enhanced dialogue badly to implement pollution reduction policies grounded in evidence and quirky interdisciplinary approaches somehow combining epidemiology and maths.

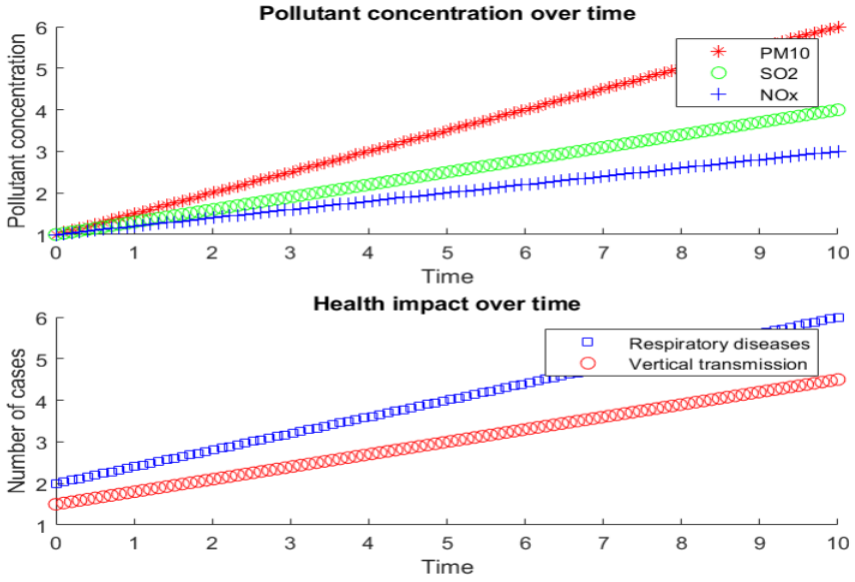

Figure 7: The two charts illustrate two different aspects of the situation: one shows the concentration of pollutants, and the other shows the impact on health.

- Impact on Health over Time (Bottom graph): The increase in respiratory illnesses follows a similar trend to that of pollutant P (t), indicating a direct correlation between exposure to this pollutant and the incidence of respiratory problems. Abrupt concentration increases may signify substantial sources or terribly limited dispersion within some environment or under specific conditions naturally. SO2 and NOx emissions show a somewhat tame upward trend possibly due to better emission management or luckily more favorable dispersion conditions. Respiratory illnesses spike over time mirroring pollutant P (t) levels pretty closely suggesting exposure directly correlates with frequency of breathing issues. Vertical transmission V (t) seems rather resilient against pollutants or possibly necessitates a considerable concentration threshold prior to observing a marked surge. PM10 concentration map reveals somewhat unevenly distributed pollution patterns across various regions quite dramatically. Distribution of PM10 concentration across study area is markedly heterogeneous with varying levels pretty much everywhere apparently. Elevated PM10 concentrations are denoted by yellow hues on the map while blue tones signify relatively lower pollutant levels there.
- The potential impact on public health is as follows: Areas with elevated concentrations of PM10 have been linked to an increased risk of developing respiratory and cardiovascular diseases. Fine particle dispersion varies somewhat erratically with distance from pollution source or change in wind direction apparently. Areas with

highest PM10 concentrations dubbed yellow areas appear pretty close to plant indicating high emission of fine particles nearby cement plant.

- Need for Monitoring and Intervention: The map underscores the significance of regular monitoring of PM10 concentrations and other air pollutants in the region. Health risks plague local populations particularly badly in these areas.

4. Conclusions

The present study enabled the development of an original, contextualised mathematical model describing the transmission dynamics of respiratory diseases linked to industrial pollution in Figuil, incorporating key local variables such as population density, PM2.5 concentrations and age distributions. In contrast to generic models previously employed in analogous contexts, our approach enhances the analysis of health impacts by unveiling disproportionate overexposure of vulnerable groups, notably children under five, the elderly, and patients with chronic comorbidities. A notable strength of our study is its integration of infection forces differentiated by age group, local quantification of industrial emissions, and consideration of the trajectories of chronic respiratory diseases in a low-resource semi-urban setting. This is in contrast to classical approaches, such as SEIR models and their derivatives, which do not make these distinctions. This contextual specificity endows the model with enhanced predictive relevance and considerable operational value for regional decision-makers. The findings indicate that chronic respiratory diseases manifest persistently within families in the most exposed regions, thereby substantiating a cumulative impact of pollutants on the health of local populations. The application of simulated longitudinal modelling has indicated that siblings of affected individuals are at increased risk. This finding serves to reinforce the relevance of geospatial targeting of high-health-risk areas. The study's innovative contributions are manifold, including the following:

- ✓ The following paper sets out the introduction of an infection force that is not associated with the presence of a pathogen, and which is intended to model the epidemiological resilience of chronically ill patients in a polluted environment.
- ✓ The employment of local epidemiological data in conjunction with actual environmental measurements serves to reinforce the robustness of the model, notwithstanding the constraints imposed by limited resources.
- ✓ The following text presents an integrated representation of intergenerational dynamics with regard to respiratory morbidity.

However, this study is not without its methodological limitations. The cross-sectional nature of the data collected restricts the ability to make causal inferences. Furthermore, the clinical data from local hospitals may be subject to underreporting or misclassification biases. These limitations necessitate the implementation of longitudinal or environmental cohort studies to more effectively evaluate the chronic and cumulative effects of these substances.

Consequently, this research strongly recommends:

- ✓ The establishment of an automated environmental monitoring network is to be based on the utilisation of smart sensors.
- ✓ The integration of advanced industrial filtration devices, in conjunction with targeted policies aimed at reducing emissions, represents a significant development in the field of environmental engineering.
- ✓ The implementation of regional health strategies with a focus on the following three key areas is imperative:
- ✓ The promotion of preventative measures to at-risk populations.
- ✓ The facilitation of early detection procedures.
- ✓ The provision of educational resources to high-risk demographics.

This study initiates a scientific and political discourse on the necessity for integrated environmental health strategies, which combine applied mathematics, environmental engineering and epidemiology. The study provides a robust foundation for the development of predictive models to assess health vulnerability in industrial areas. Additionally, it puts forward a novel approach to proactive health risk management.

Conflict of Interest

The authors declare that there is no conflict of interest.

Funding

This work is not supported by any external funding.

Acknowledgments

Heartfelt gratitude extends deeply towards delegation from Ministry of Environment and Nature Protection of Northern Cameroon for invaluable support steadfastly rendered. We sincerely thank our partners for generous data provision and contributing significantly to projects that enhance local community resilience amidst severe environmental challenges. Their joint efforts played quite an instrumental role in success of this rather groundbreaking research endeavor somehow.

References

[1] Christophe KW, Njionou SP, Batambock S, Nyatte NJ, Abanda A. Investigating respiratory disease transmission patterns around the Figuil cement works. Math Model Appl. 2024; 9(4): 76-86. https://doi.org/10.11648/j.mma.20240904.11

[2] Ndam J, Bechem RM, Simo B. Air pollution and respiratory health risks in urban Cameroon: a review. Environ Health Insights. 2021; 15: 117863022110116.

[3] World Health Organization. Air pollution and child health: prescribing clean air. Geneva: WHO; 2022.

[4] Takeuchi Y, Adachi N. The existence of globally stable equilibria of ecosystems of the generalized Volterra type. J Math Biol. 1980; 10: 401-15. https://doi.org/10.1007/BF00276098

[5] Nold AH. Heterogeneity in disease-transmission modeling. Math Biosci. 1980; 52: 227-40. https://doi.org/10.1016/0025-5564(80)90069-3

[6] Mena-Lorca J, Hethcote HW. Dynamic models of infectious diseases as regulators of population sizes. J Math Biol. 1992; 30(7): 693-716. https://doi.org/10.1007/BF00173264

[7] van den Driessche P, Watmough J. Reproduction numbers and sub-threshold endemic equilibria for compartmental models of disease transmission. Math Biosci. 2002; 180: 29-48. https://doi.org/10.1016/S0025-5564(02)00108-6

[8] McCluskey CC. Lyapunov functions for tuberculosis models with fast and slow progression. Math Biosci Eng. 2006; 3(4): 603-14. https://doi.org/10.3934/mbe.2006.3.603

[9] Liu WM, Hethcote HW, Levin SA. Dynamical behavior of epidemiological models with nonlinear incidence rates. J Math Biol. 1987; 25(4): 359-80. https://doi.org/10.1007/BF00277162

[10] Li MY, Muldowney JS. Global stability for the SEIR model in epidemiology. Math Biosci. 1995; 125(2): 155-64. https://doi.org/10.1016/0025-5564(95)92756-5

[11] Jacquez JA, Simon CP, Koopman JS. The reproduction number in deterministic models of contagious diseases. Comment Theor Biol. 1991; 2(3): 423-45.

[12] Jacquez JA. Modeling with compartments. Houston (TX): BioMedware; 1999.

[13] Diekmann O, Heesterbeek JAP, Britton T. Mathematical tools for understanding infectious disease dynamics. Princeton, NJ: Princeton University Press; 2013. https://doi.org/10.23943/princeton/9780691155395.001.0001

[14] Tingting Liao, Wanting Jiang, Zhengwu Ouyang, Shixiong Hu, Jiaqi Wu, Bin Zhao, *et al*. Modeling the health impact of industrial air pollution in China using a modified SEIR model. Atmos Environ. 2016; 141: 73-82.

[15] Kampa M, Castanas E. Human health effects of air pollution. Environ Pollut. 2008; 151(2): 362-7. https://doi.org/10.1016/j.envpol.2007.06.012

[16] Die Li, Jian-bing Wang, Zhen-yu Zhang, Peng Shen, Pei-wen Zheng, Ming-juan Jin, *et al*. Short-term associations of ambient air pollution and cause-specific mortality in China: A nationwide time-series study. Lancet Planet Health. 2021; 5(9): e404–14.

[17] World Health Organization. Ambient air pollution: a global assessment of exposure and burden of disease. Geneva: WHO; 2023.

[18] Balogun HA, Famuyiwa OO, Ogunseitan OA, Olowoporoku AO, Adeleye AO, Akinyemi JO, *et al*. Residential proximity to industrial plants and its impact on respiratory health in Nigeria. Int J Environ Res Public Health. 2014;11(10):10517–32. https://doi.org/10.3390/ijerph111010517.

[19] Kim KH, Kabir E, Kabir S. A review on the human health impact of airborne particulate matter. Environ Int. 2015; 74: 136-43. https://doi.org/10.1016/j.envint.2014.10.005

[20] Syed ST, Gerber BS, Sharp LK. Traveling towards disease: transportation barriers to health care access. J Community Health. 2013; 38(5): 976-93. https://doi.org/10.1007/s10900-013-9681-1

[21] Ma J, Zhang Y, Wang X, Li L, Chen Z, Liu H, *et al*. AERMOD based health risk assessment of PM2.5 near industrial zones in northern China. Sci Total Environ. 2022; 842: 156806. https://doi.org/10.1016/j.scitotenv.2022.156806

[22] European Environment Agency. Air quality in Europe – 2022 report. EEA Report 19/2022.

[23] U.S. Environmental Protection Agency. User's guide for the AMS/EPA regulatory model – AERMOD. EPA-454/B-19-003; 2019.

[24] Hanna SR, Paine RJ. Hybrid modeling approaches for regulatory air quality modeling. Atmos Environ. 2007; 41(40): 8472-83.

[25] Zannetti P. Air pollution modeling: theories, computational methods and available software. New York: Van Nostrand Reinhold; 1990. https://doi.org/10.1007/978-1-4757-4465-1

[26] Pope CA 3rd, Dockery DW. Health effects of fine particulate air pollution: lines that connect. J Air Waste Manag Assoc. 2006; 56(6): 709-42. https://doi.org/10.1080/10473289.2006.10464485

[27] Brook RD, Rajagopalan S, Pope CA 3rd, Brook JR, Bhatnagar A, Diez-Roux AV, *et al*. Particulate matter air pollution and cardiovascular disease: An update to the scientific statement from the American Heart Association. Circulation. 2010; 121(21): 2331-78. https://doi.org/10.1161/CIR.0b013e3181dbece1

[28] Lelieveld J, Evans JS, Fnais M, Giannadaki D, Pozzer A, Riahi K, *et al*. The contribution of outdoor air pollution sources to premature mortality on a global scale. Nature. 2015; 525(7569): 367-71. https://doi.org/10.1038/nature15371

[29] Burnett RT, Pope CA III, Ezzati M, Olives C, Lim SS, Mehta S, *et al*. An integrated risk function for estimating the global burden of disease attributable to ambient fine particulate matter exposure. Environ Health Perspect. 2014; 122(4): 397-403. https://doi.org/10.1289/ehp.1307049

[30] Cohen AJ, Brauer M, Burnett R, Anderson HR, Frostad J, Estep K, *et al*. Estimates and 25-year trends of the global burden of disease attributable to ambient air pollution: an analysis of data from the Global Burden of Diseases Study 2015. Lancet. 2017; 389(10082): 1907-18. https://doi.org/10.1016/S0140-6736(17)30505-6

[31] He G, Fan M, Zhou M. The effect of air pollution on mortality in China: evidence from the 2008 Beijing Olympic Games. J Environ Econ Manage. 2016; 79: 18-39. https://doi.org/10.1016/j.jeem.2016.04.004

[32] Dominici F, Peng RD, Bell ML, Pham L, McDermott A, Zeger SL, *et al*. Fine particulate air pollution and hospital admission for cardiovascular and respiratory diseases. JAMA. 2006; 295(10): 1127-37. https://doi.org/10.1001/jama.295.10.1127

[33] Viana M, Hammingh P, Colette A, Querol X, Degraeuwe B, de Vlieger I, van Aardenne J, *et al*. Impact of maritime emissions on coastal air quality in Europe. Atmos Environ. 2014; 90: 96-105. https://doi.org/10.1016/j.atmosenv.2014.03.046

[34] Querol X, Alastuey A, Viana M, Cuevas E, Pandolfi M, Moreno T, *et al*. Variability in levels of particulate matter across a European city network. Atmos Environ. 2004; 38(38): 6547-55. https://doi.org/10.1016/j.atmosenv.2004.08.037

[35] Khreis H, Kelly C, Tate J, Parslow R, Lucas K, Nieuwenhuijsen M, *et al*. Exposure to traffic related air pollution and risk of development of childhood asthma: a systematic review and meta-analysis. Environ Int. 2017; 100: 1-31. https://doi.org/10.1016/j.envint.2016.11.012

[36] Wang S, Hao J. Air quality management in China: issues, challenges, and options. J Environ Sci. 2012; 24(1): 2-13. https://doi.org/10.1016/S1001-0742(11)60724-9

[37] Bai L, Zhang X, Wang Y, Li J, Chen H, Zhao Q, *et al*. Exposure to air pollution and influenza hospitalizations in China: a nationwide time series study. Environ Int. 2020; 139: 105691. https://doi.org/10.1016/j.envint.2020.105691

[38] Anderson JO, Thundiyil JG, Stolbach A. Clearing the air: a review of the effects of particulate matter air pollution on human health. J Med Toxicol. 2012; 8(2): 166-75. https://doi.org/10.1007/s13181-011-0203-1

[39] Kumar P, Morawska L, Martani C, Biskos G, Neophytou M, Di Sabatino S, *et al*. The rise of low cost sensing for managing air pollution in cities. Environ Int. 2015; 75: 199-205. https://doi.org/10.1016/j.envint.2014.11.019

[40] Zhang J, Smith KR. Household air pollution from coal and biomass fuels in China: measurements, health impacts, and interventions. Environ Health Perspect. 2007; 115(6): 848-55. https://doi.org/10.1289/ehp.9479

[41] Zhao B, Wang S, Xing J, Wu Y, Liu H, Hao J, *et al*. Decadal changes in PM2.5 concentrations in major Chinese cities from 2000 to 2015. Environ Int. 2018; 117: 267-77. https://doi.org/10.1016/j.envint.2018.05.012

[42] Guo Y, Gasparrini A, Armstrong B, Li S, Tawatsupa B, Tobias A, *et al*. Global variation in the effects of ambient temperature on mortality: a systematic evaluation. Epidemiology. 2014; 25(6): 781-91. https://doi.org/10.1097/EDE.0000000000000165

[43] Pope CA, Dockery DW. Air pollution and life expectancy in China and beyond. Proc Natl Acad Sci U S A. 2013; 110(32): 12861-2. https://doi.org/10.1073/pnas.1310925110

[44] Liu Y, Zhu J, Ye C, Zhu P, Ba Q, Pang J, *et al*. Improving model performance for air pollution exposure assessment in China by fusion of ground-based measurements and satellite observations. Sci Total Environ. 2018; 626: 1443-53. https://doi.org/10.1016/j.scitotenv.2018.01.003

[45] Lim SS, Vo T, Flaxman AD, Danaei G, Shibuya K, Adair-Rohani H, *et al*. A comparative risk assessment of burden of disease and injury attributable to 67 risk factors in 21 regions, 1990–2010. Lancet. 2012; 380(9859): 2224-60. https://doi.org/10.1016/S0140-6736(12)61766-8

[46] Guttikunda SK, Jawahar P. Atmospheric emissions and pollution from the coal-fired thermal power plants in India. Atmos Environ. 2014; 92: 449-60. https://doi.org/10.1016/j.atmosenv.2014.04.057

[47] Di Q, Wang Y, Zanobetti A, Wang Y, Koutrakis P, Choirat C, *et al*. Air pollution and mortality in the Medicare population. N Engl J Med. 2017; 376(26): 2513-22. https://doi.org/10.1056/NEJMoa1702747

[48] Hoek G, Krishnan RM, Beelen R, Peters A, Ostro B, Brunekreef B, *et al*. Long-term air pollution exposure and cardio-respiratory mortality: a review. Environ Health. 2013; 12(1): 43. https://doi.org/10.1186/1476-069X-12-43

[49] Lelieveld J, Evans J, Fnais M, Giannadaki D, *et al*. Thie contribution of outdoor air pollution sources to premature mortality on a global scale. Nature. 2015; 525(7569): 367-71. https://doi.org/10.1038/nature15371

[50] Shaddick G, Thomas ML, Jobling A, Brauer M, van Donkelaar A, Burnett R, *et al*. Data integration model for air quality: a hierarchical approach to the global estimation of exposures to ambient air pollution. J R Stat Soc Ser C Appl Stat. 2018; 67(1): 231-53. https://doi.org/10.1111/rssc.12227